Hyperspectral imaging and machine learning for the prediction of SSC in kiwi fruits

Jon Elias Moen ∗, Vebjørn Nilsen, Katherine Brox Saidi, Eivind Kohmann,
Binu Melit Devassy, and Sony George

The Norwegian Colour and Visual Computing Laboratory, Department of Computer
Science, Norwegian University of Science and Technology, Gjøvik 2802, Norway
∗ Correspondence: jon.elias.moen@gmail.com

Abstract. Hyperspectral imaging of kiwi fruits was performed, to study the Soluble Solids Content (SSC) of the fruits in a non-destructive way. A database is created which includes the hyperspectral data acquired in the visible and near-infrared region (VNIR) and measurements done with a sugar meter. We have applied different machine learning techniques to investigate the correlation between spectral information and the SSC. The models tested were support vector regression (SVR), k-nearest neighbor (KNN), partial least squares (PLS), and multiple linear regression (MLR) with different variable selection techniques and dimensionality reduction. The best model at determining SSC was Uninformative Variable Elimination (UVE)-PLS, which had RMSE = 1.047 °Brix and R^2 = 0.39 on the test set.

1 Introduction

Hyperspectral imaging (HSI) is used in several sectors like agriculture [17], medicine [29], forensic [18], remote sensing [8], food [11] and material analysis [19]. A compelling reason for using HSI is because it acts non-destructively on objects, as it only uses the reflectance property for analysis. Thus, it is not coincidental that the number of scientific papers involved with HSI has increased significantly in the last few years, and the trend seems to continue[23].

In recent years, food has received a lot of attention within the hyperspectral imaging science community[5][24]. The purpose of this paper is to further examine how HSI can be used to determine the Soluble Solids Content (SSC) and maturity of kiwi fruits using the the VNIR spectral range. This has been shown to be possible by Li et al. 2019 [16] and Berardinelli et al. 2019 [3]. This was achieved by collecting physical measurements and hyperspectral data of 495 kiwis, the creation of automatic labeling software, and regression and machine learning models. If such research were to be commercialized, a huge amount of food waste would be reduced and large parts of the harvesting process could be automated, according to ImpactVision [26].

1.1   State of the art

The relationships between SSC (measured by refractometer), kiwifruit ripeness, and eating quality was an interesting point of investigation for many researchers. Ford and his research team[6] in 1971 found that "Hayward" kiwifruit harvested having SSC less than 6.0° Brix (indicating the percentage of sugar contents in the fruit) did not give a good flavor when ripe. Other researchers started also to work on this subject and based on their findings lead to a regulation that harvesting of "Hayward" kiwi can be done when these have reached a minimum of 6.2° Brix. All this to ensure the best quality and maturity for the customers.

There have been several successful attempts at evaluating SSC non-destructively in "Hayward" kiwi using spectroscopy operating in the VNIR range. Moghimi (2010) [21] investigated "Hayward" kiwi spectra in transmission mode in the range 400-1000nm. Using PLS to predict SSC, they achieved a R^2 of 0.93 and root mean square error of prediction (RMSEP) of 0.259° Brix using Standard Normal Variate (SNV) combined with median filter and the first derivative. RMSEP is used as an indicator of the reliability and predictive ability of the models. Lee et al.(2012)[14] used a modified version of PLS to predict SSC in the 400-2500nm spectral range and got standard error of prediction (SEP) of 0.49° Brix and with R^2 of 0.98. These papers have achieved good performance but are captured using spectroscopy, which has drawbacks. The spectral information is only obtained from a single point or a very small area of the fruit and are not feasible for scanning multiple fruits at a faster rate. As hyperspectral imaging solves this problem by combining conventional imaging with spectroscopy.

Hyperspectral imaging have been used to evaluate SSC in several fruits, such as blueberries (Qiao et al. 2019 [25]) , cherries (Li et al. (2018) [15]) , oranges (Riccioli et al. 2021) [27]. These studies show that hyperspectral imaging has the ability to predict SSC in fruits in a non-destructive manner. However, there is little research using hyperspectral imaging to determine SSC in kiwis. Guo et al.(2016) [9] studied the kiwi varieties "Xixuan" and "Huayou" in the spectral range 865–1711nm and got R^2 0.766 and 0.971 and RMSEP 0.968 and 0.589° Brix, respectively. One study on "Hayward" kiwifruit (Hu et al. 2017 [10]) looked into determining glucose, fructose and sucrose in the 400-1000nm spectral range, which achieved a score R^2 in the range 0.64-0.5, using PLSR and LSSVM.

As there exist not much research on determining SSC in "Hayward" kiwifruit using hyperspectral imaging, the goal of the present study is to look into the possibilities of determining SSC in "Hayward" kiwi by using regression and machine learning models.

2   Materials & Method

2.1   Kiwi Samples

The kiwi fruit samples used in this paper are of the type Hayward delivered by Bama AS. A total number of 495 kiwis were scanned in 9 batches of 55 kiwis in each batch for 3 weeks (see table 1). The physiological measurement

was conducted shortly after the hyperspectral acquisition. The kiwi fruits were stored at 8°C in the scanning week, and at 4°C otherwise.

Table 1: Weekly plan of scanning and destructive measurements.

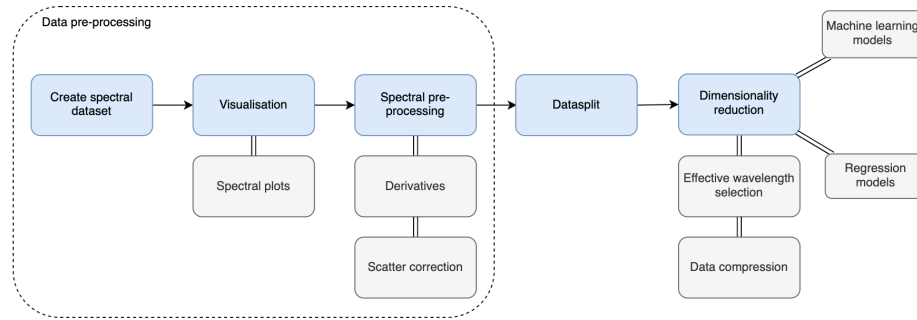|		Imaging (HSI)	Physiological measurements and RGB imaging
	Day 1	Box 1, Box 2, Box 3	Box 1
Week 1	Day 2	Box 2, Box 3	Box 2
	Day 3	Box 3	Box 3
	Day 1	Box 4, Box 5, Box 6	Box 4
Week 2	Day 2	Box 5, Box 6	Box 5
	Day 3	Box 6	Box 6
	Day 1	Box 7, Box 8, Box 9	Box 7
Week 3	Day 2	Box 8, Box 9	Box 8
	Day 3	Box 9	Box 9

2.2 Data acquisition

Fig. 1: The steps involved in pre-processing HS data before using it to train models.

The camera used in this paper was a HySpex-VNIR-1800, produced by Norsk Elektro Optikk AS (`https://www.hyspex.com/`). The specs of the camera are listed in table 2. The camera is of type push-broom and was placed 30cm away from the kiwis when scanning. The halogen light sources were angled at 45° to a moving conveyor belt where the kiwis were placed. Figure 2 illustrates the setup.

The destructive measurements of SSC were conducted by slicing and squeezing the kiwis to get juice droplets into a Brix-refractometer of type Digital Atago Pal-1.

The data acquisition created 495 SSC measurements corresponding to hyperspectral images of 495 kiwis. The images had two spatial dimensions X and Y, with a spectral dimension Z (see figure 3).

Table 2: Important specifications of VNIR-1800

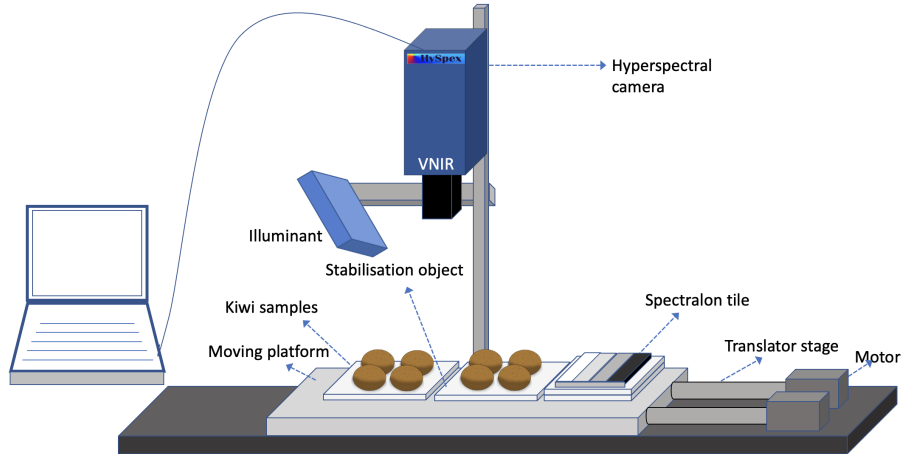|	HySpex VNIR-1800
Sensitivity range (nm)	400-1000
Spatial pixels	1800
Spectral sampling (nm)	3.26
Spectral channels	186
Bit depth	16
Sensor type	CMOS
Field of view	$17°$
Max speed (fps)	260

Fig. 2: Our setup with a hyperspectral camera, illuminant, conveyor belt with moving platform, spectralon tile, and kiwis on a stable surface.

2.3   Pre-processing

The entire pre-processing workflow is illustrated in figure 1.

The acquired HSI data was pre-processed through several steps to remove redundant information. The HSI images were first corrected by subtracting the dark current and normalized by translating each pixel value from radiance to
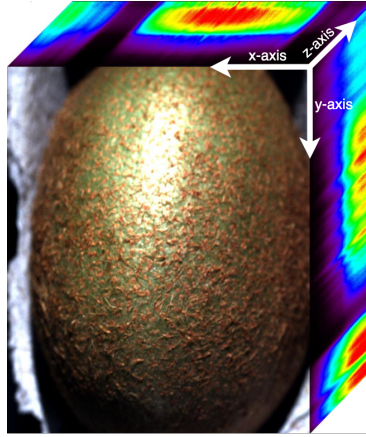
Fig. 3: Spectral data (datacube) of a kiwi where the x- and y-axis representing the spatial dimensions and the z-axis the spectral dimension.

reflectance. This resulted in more comparable results between scanning batches as kiwis do not always have the same shape and height.

After normalization, two spectral datasets were created using the average spectrum of the whole kiwi and the average spectrum on a 150x150 pixel area in the center of each kiwi. These areas were found by using an automatic spectra collector algorithm that classifies kiwis in the image. After that, a Hanning window filter was applied to improve the signal to noise ratio (SNR).

Pre-processing was applied to both the spectral datasets and Brix values. A 99% confidence interval was used to remove outliers from the Brix data range. Then, spectral pre-processing was performed to smooth out the spectra of the remaining samples.

The spectral pre-processing techniques used were SNV, multiplicative scatter correction (MSC), Hanning window, and derivatives using the Savitzky-Golay filter[28], which are regularly used when working with spectral data[22]. To find what pre-processing worked best for each model, each model was tested with and without and a combination of SNV or MSC with different degrees of derivatives. This was carried out on the models by brute force. In other words all these different combinations were applied iteratively on the models, and by measuring the model performance; the best pre-processing combination was found.To find the efficient wavelengths for predicting sugar, we used several feature elimination methods. These are more explained with the models.

2.4   Data split

To ensure that our models would be able to predict a wide range of values, we used the sample set partitioning based on joint x-y distance (SPXY) algorithm proposed by Galvão [7]. It takes into account the variability in both X- and

Y-spaces when dividing the data into calibration and prediction sets and was shown to be advantageous for especially PLS. SPXY was used twice to split the dataset into 4 smaller ones. Before the split, we discarded samples outside of a 99% confidence interval, reducing the number of kiwis in the dataset down to 444. The SPXY algorithm was first used to create a calibration and a prediction set with a 7 : 3 distribution as illustrated in figure 4. The prediction set was further split into validation and verification using the same algorithm but with a 1 : 1 distribution. It is important to note that the dataset split was applied after any spectral pre-processing. The calibration and verification datasets have values spanning over the most extended range since they are being used to train and test each model.
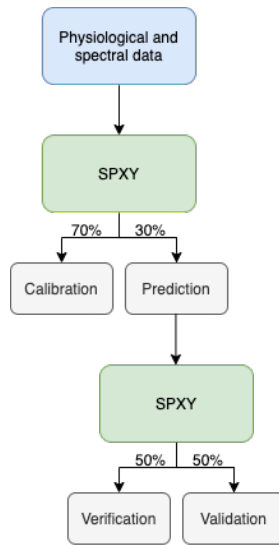
Fig. 4: The construction of the different datasets using SPXY.

2.5   Models

Several machine learning and regression models were applied and evaluated. To evaluate these models, R^2(coefficient of determination which is a measure representing how close the data are to the fitted regression line) and RMSE(Root-mean-square error which is used to measure the differences between values predicted by a model) were used as performance measures and tested on different datasets. Details about these are discussed below. The models try to predict the wavelengths correlation with the variation in SSC.

Training & evaluation Pipeline cross-validation was used to find the best hyperparameters for each model. The cross-validation performance metrics were

R^2 and RMSE . The models' performance on the verification and validation datasets were compared to the calibration dataset performance to make sure the models were not overfitted.

Support vector regression (SVR) In SVR we want to define a margin of error, ϵ, for the regression function to decrease how strictly the hyperplane fits the data points. As we most likely cannot include all data points within the margin of error, we need to include another variable, ξ, to measure the error of all points outside the margin of error. This works well in specific datasets as there is often a margin of error in real-world data, and the points outside the margin of error can be viewed as noise or outliers. With the constraints ϵ and ξ, we can define our boundaries for the hyperplane:

$$|y_i - w_i x_i| \leq \epsilon + |\xi_i| \tag{1}$$

So with the constraints in mind, we want to minimize the Euclidean distance $MIN(\frac{1}{2}||w||^2)$ of the data points to the margin of error. We can minimize w and add a constant C to scale the dependence of the sum of errors of the points outside of the margin of error:

$$MIN(\frac{1}{2}||w||^2) + C \sum_{i=1}^{n} \xi_i$$

There is a large margin of error between different kiwis and scanning period, making SVR interesting compared to ordinary linear regression. The margin of error and weight of points outside the margin of error can be tuned, and thus brings more hyperparameters that can influence results in various ways, making SVR a good candidate model.

K-nearest neighbors regression (KNN-r) KNN-r is based on the classification algorithm KNN where the dependent values are predicted based on the training of independent variables by determining the k closest data points and interpolating. KNN-r works well with few data points as it does not use all values to predict, and can be tuned with hyperparameters like values of k and different distance function methods through cross-validation. As KNN-r uses few data points for interpolation of predicted values, it can be effective in real-time applications where the kiwi predictions need to be processed rapidly.

Partial least squares (PLS) PLS is an efficient regression method based on covariance. It is recommended to be used in cases of regression where the number of explanatory variables is high, and where it is likely that the these variables are correlated. This regression method works similarly to Principal component regression (PCR, which is often used to estimate the unknown regression coefficients in a linear regression model), and is broadly used for this application [22].

It works well on spectra because it eliminates multicollinearity, which means that the independent variables can vary with each other.

In broad terms PLS works by computing the principal components of both the independent and dependent variable and perform least-squares on these components instead.

The Efficient variable selection algorithms Uninformative Variable Elimination (UVE)[4][20] and Genetic algorithm (GA)[30][13] were applied together with PLS. These algorithms were used to exclude wavelengths that did not contribute a significant amount to the prediction.

Multiple linear regression (MLR) Multiple linear regression is an extension of linear regression but with more explanatory components. It assumes the relationship between the dependent variable Y and independent variable X is linear and can be approximated using equation 2.

$$Y = \beta_0 + \beta_1 X_{i,0} + \beta_2 X_{i,1} + ..\beta_n X_{i,n} + \epsilon_i \qquad (2)$$

where β_n is an unknown coefficient for each independent variable except β_0 which is the y-intersect, n is the number of bands, i represents a sample and ϵ is the predicted error. The objective of the function is to find certain β values such that it minimizes the error, which we calculate using the root mean square error (RMSE). The equation is primarily solved using Ordinary least squares (OLS)[12] and was also used in this work.

MLR was combined with the successive projections algorithm (SPA)[2] for wavelength selection, but also with elimination methods such as F-test to further reduce the number of wavelengths used in the following paper [1].

3   Results and Discussion

In the box-plot of physical measurements (see figure 5) we can see that the Soluble Solids Content (SSC) increases steadily, which is expected as the kiwis mature over time. Discussion about the model's performance in predicting these values by kiwi spectrum will come later in this section.

The SPA-MLR model was chosen based on the validation dataset performance across the different efficient wavelengths selected by the SPA algorithm, as it has no tunable parameters. The performance was medium as it resulted in the best overall R^2 of 0.405 and 1.11 RMSE on the verification set and had similar values for the calibration values. The other models had their parameters tuned for the final model using cross-validation, not using the validation dataset for tuning. All final models were tested on the same dataset (verification) to ensure that they were comparable to each other.

The optimal spectral pre-processing for each model was carried out by testing several different permutations with and without MSC or SNV and Savitzky-Golay filter. The parameters tested in the Savitzky-Golay filter were derivatives of the degree 0-2, window size 7-33, and fitting polynomial 3-5. The models were
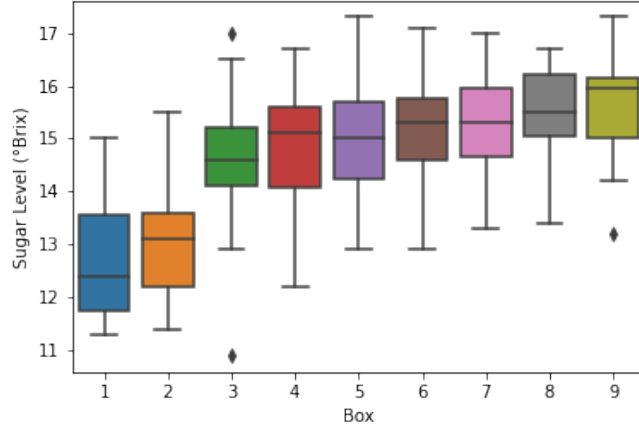
Fig. 5: SSC from the 9 days of measurements, where each box (day) has its own color.

compared based on their performance regarding RMSE, R^2 and the amount of EWs on the training (calibration) and verification set.

Table 3 shows that UVE-PLS obtained medium accuracy at predicting SSC with medium-to-low RMSEC and RMSEV, and similar R_C^2 and R_V^2 on the dataset using the whole kiwi (Full). SPA-MLR seems to perform equally well but uses a larger group of wavelengths instead of more distinct wavelengths spread out like in UVE-PLS. As UVE-PLS needs the least amount of EWs to predict as close to equal as SPA-MLR, it is considered the slightly better model of the ones that were tested.

In comparison to approaches using spectroscopy, our models performed generally poorer. One significant similarity is that Moghimi (2010)[21] used the same spectral pre-processing, SNV, and first derivative using Savitzky-Golay on "Hayward" kiwi but their data from spectroscopy. This gives some confirmation that SNV and the first derivative are good for pre-processing "Hayward" kiwi spectra when trying to predict SSC.

The wavelengths used in the final SPA-MLR and UVE-PLS model both included small packets of wavelengths which can be seen in figure 6. This is very clear in figure 6b as SPA-MLR used every captured wavelength between 682-736nm (18 distinct wavelengths). This could mean that the internal chemical changes in the kiwi that correlates with the SSC affect a wide range of wavelengths, and in several regions. There is no clear distinction of which wavelengths are the most important as the two models only share one common wavelength for prediction. Although these are two different models, it would be expected that they used more common wavelengths, as they both are trying to predict

SSC

Camera	Dataset	Model	Pre-processing	EWs	RMSE_C	RMSE_V	R^2_C	R^2_V
VNIR	Full	SPA-MLR	SNV SavitzkyGolay(27,5,1)	21	1.343	1.11	0.397	0.405
		UVE-PLS	SNV SavitzkyGolay(27,5,1)	16	1.308	1.047	0.428	0.39
		GA-PLS	SavitzkyGolay(45,2,2)	86	2.783	1.669	0.097	0.156
		KPCA-SVR	StandardScaler	comp=41	1.109*	1.141*	0.682	0.24
		KPCA-KNN	MSC, SavitzkyGolay(31,2,0)	178	1.082*	0.779*	0.068	0.062
	Region	SPA-MLR	SNV SavitzkyGolay(21,5,2)	33	1.364	1.131	0.376	0.371
		UVE-PLS	SNV SavitzkyGolay(27,5,1)	20	1.352	1.1	0.381	0.314
		GA-PLS	MSC SavitzkyGolay(49,2,1)	86	1.078	0.989	0.231	0.111
		KPCA-SVR	StandardScaler	comp=59	0.878*	1.24*	0.813	0.216
		KPCA-KNN	SNV, SavitzkyGolay(39,5,2)	17	0.952*	0.939*	0.171	0.191

Table 3: The best performances of each model for evaluating Soluable Solids Content (SSC) in the Visable and near-infrared (VNIR) range on the two different datasets, Full (average of whole kiwi) and Region (150x150 averaged area). Every model used the same calibration (70%) and verification (15%) set. (* KPCA-SVR and KPCA-KNN uses StandardScaler, therefore the RMSE value of this models is not directly comparable).

(a) Efficient wavelengths: 717, 739-745, 758-771, 806-819, 835-838nm

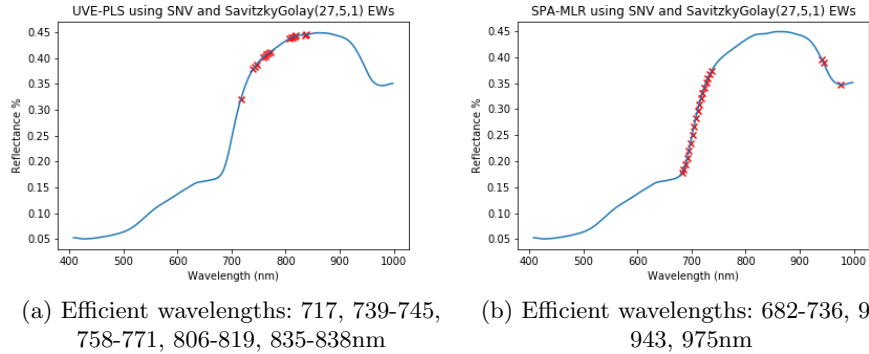(b) Efficient wavelengths: 682-736, 940, 943, 975nm

Fig. 6: The resulting efficient wavelengths that performed best at predicting SSC in the two models.

SSC. This blurs the indication of which wavelengths are good predictors, making it difficult to use these models in a simpler system, e.g. a multispectral system.

The results could be impacted by some sources of error in the data acquisition period. There is a chance that some values were measured wrong because of external noise or internal deviation in the measurement device. It is also possible that the results could have improved with a larger dataset as there is variance in kiwi samples. Another important factor to recognize is that the harvest date, days in transit, and the temperature in these circumstances are unknown. This creates greater uncertainty in the actual maturity of the kiwis at the different scanning days, which can impact the rate of maturation within the acquisition period. Lower bio-variability makes it harder for the models to generalize for the

different maturity stages for the 'Hayward' kiwis, and might also not be stable for kiwis with defects or other differentiating factors such as soil type and season.

The scanning speed with the HSI method used in this paper is fast, but the efficiency improvement comes with a drop in R^2 of 0.5, meaning that this exact model would not be accurate enough for commercialization. By improving or eliminating the sources of error, the drop would become less significant and the efficiency trade-off would become more desirable for commercial usage.

4   Conclusion

The model that achieved the highest accuracy was SPA-MLR with R^2 of 0.405 and 1.11° Brix RMSE on the verification set. It had low variance between training and testing results, indicating no overfitting. UVE-PLS obtained a lower R^2 of 0.39 but had a smaller RMSE of 1.047° Brix using fewer wavelengths. More work on the dataset like reducing or eliminating sources of error, would likely increase the performance of the models.

It was found that applying spectral pre-processing methods such as SNV and first derivative increased the model performance in determining SSC in kiwi of type "Hayward". MSC did not perform equally good.

These findings show that non-destructive determination of SSC in kiwi of type "Hayward" is possible in the VNIR range using a hyperspectral camera but more research is needed to establish a good model that can be used as quality control in the food industry. By improving the performance of the model enough for commercialisation, efficiency in the industry would increase, and less food would be wasted in destructive measurements.

5   Author contribution

All authors of this study have contributed equally. S.G training and supervision; E.K, V.N and J.M methodology; K.S research; All members except S.G writing, review, and editing. B.D Review, Experimental support.

References

1.
2. Araújo, M.C.U., Saldanha, T.C.B., Galvão, R.K.H., Yoneyama, T., Chame, H.C., Visani, V.: The successive projections algorithm for variable selection in spectroscopic multicomponent analysis. Chemometrics and Intelligent Laboratory Systems **57**(2), 65–73 (2001). https://doi.org/10.1016/S0169-7439(01)00119-8
3. Berardinelli, A., Benelli, A., Tartagni, M., Ragni, L.: Kiwifruit flesh firmness determination by a NIR sensitive device and image multivariate data analyses. Sens. Actuators, A **296**, 265–271 (Sep 2019). https://doi.org/10.1016/j.sna.2019.07.027
4. Centner, V., Massart, D.L., de Noord, O.E., de Jong, S., Vandeginste, B.M., Sterna, C.: Elimination of uninformative variables for multivariate calibration. Anal. Chem. **68**(21), 3851–3858 (Nov 1996). https://doi.org/10.1021/ac960321m

5. Devassy, B., George, S.: Estimation of strawberry firmness using hyperspectral imaging: a comparison of regression models. Journal of Spectral Imaging (Jun 2021). https://doi.org/10.1255/jsi.2021.a3

6. Ford, J.: Harvesting and maturity of chinese gooseberries. Orchardist NZ (1971)

7. Galvão, R.K.H., Araujo, M.C.U., José, G.E., Pontes, M.J.C., Silva, E.C., Saldanha, T.C.B.: A method for calibration and validation subset partitioning. Talanta **67**(4), 736–740 (2005). https://doi.org/10.1016/j.talanta.2005.03.025

8. Goetz, A.F.: Three decades of hyperspectral remote sensing of the earth: A personal view. Remote Sensing of Environment **113**, S5–S16 (2009). https://doi.org/10.1016/j.rse.2007.12.014, imaging Spectroscopy Special Issue

9. Guo, W., Zhao, F., Dong, J.: Nondestructive Measurement of Soluble Solids Content of Kiwifruits Using Near-Infrared Hyperspectral Imaging. Food Anal. Methods **9**(1), 38–47 (Jan 2016). https://doi.org/10.1007/s12161-015-0165-z

10. Hu, W., Sun, D.W., Blasco, J.: Rapid monitoring 1-mcp-induced modulation of sugars accumulation in ripening 'hayward' kiwifruit by vis/nir hyperspectral imaging. Postharvest Biology and Technology **125**, 168–180 (2017). https://doi.org/10.1016/j.postharvbio.2016.11.001

11. Huang, H., Liu, L., Ngadi, M.O.: Recent developments in hyperspectral imaging for assessment of food quality and safety. Sensors **14**(4), 7248–7276 (2014). https://doi.org/10.3390/s140407248

12. Hutcheson, G.D.: Ordinary Least-Squares Regression. In: The Multivariate Social Scientist (1999), `http://doi.org/10.4135/9780857028075`

13. Leardi, R.: Application of genetic algorithm–PLS for feature selection in spectral data sets. J. Chemom. **14**(5-6), 643–655 (Sep 2000). https://doi.org/10.1002/1099-128X(200009/12)14:5/6¡643::AID-CEM621¿3.0.CO;2-E

14. Lee, J.S., Kim, S.C., Seong, K.C., Kim, C.H., Um, Y.C., Lee, S.K.: Quality Prediction of Kiwifruit Based on Near Infrared Spectroscopy. Horticultural Science & Technology **30**(6), 709–717 (2012). https://doi.org/10.7235/hort.2012.12139

15. Li, X., Wei, Y., Xu, J., Feng, X., Wu, F., Zhou, R., Jin, J., Xu, K., Yu, X., He, Y.: Ssc and ph for sweet assessment and maturity classification of harvested cherry fruit based on nir hyperspectral imaging technology. Postharvest Biology and Technology **143**, 112–118 (2018). https://doi.org/10.1016/j.postharvbio.2018.05.003

16. Li, X., Li, R., Wang, M., Liu, Y., And, B.Z.: Hyperspectral Imaging and Their Applications in the Nondestructive Quality Assessment of Fruits and Vegetables (Dec 2017). https://doi.org/10.5772/intechopen.72250

17. Melit Devassy, B., George, S.: Comparison of ink classification capabilities of classic hyperspectral similarity features. In: 2019 International Conference on Document Analysis and Recognition Workshops (ICDARW). vol. 8 (2019), `http://ceur-ws.org/Vol-2688/paper9.pdf`

18. Melit Devassy, B., George, S.: Forensic analysis of beverage stains using hyperspectral imaging - Scientific Reports. Sci. Rep. **11**(6512), 1–13 (Mar 2021). https://doi.org/10.1038/s41598-021-85737-x

19. Melit Devassy, B., George, S., Hardeberg, J.Y.: Contactless classification of strawberry using hyperspectral imaging. In: CEUR Workshop Proceedings. vol. 2688, pp. 25–30 (2020). https://doi.org/10.1109/ICDARW.2019.70137

20. Mendoza, F., Lu, R.F., Ariana, D., Cen, H.Y., Bailey, B.: Integrated spectral and image analysis of hyperspectral scattering data for prediction of apple fruit firmness and soluble solids content. Postharvest Biol. Technol. **62**(2), 149–160 (2011), `https://www.cabdirect.org/cabdirect/abstract/20113338024`

21. Moghimi, A., Aghkhani, M.H., Sazgarnia, A., Sarmad, M.: Vis/nir spectroscopy and chemometrics for the prediction of soluble solids content and acidity (ph) of kiwifruit. Biosystems Engineering **106**(3), 295–302 (2010). https://doi.org/10.1016/j.biosystemseng.2010.04.002

22. Nicolaï, B.M., Beullens, K., Bobelyn, E., Peirs, A., Saeys, W., Theron, K.I., Lammertyn, J.: Nondestructive measurement of fruit and vegetable quality by means of NIR spectroscopy: A review. Postharvest Biol. Technol. **46**(2), 99–118 (Nov 2007). https://doi.org/10.1016/j.postharvbio.2007.06.024

23. Polder, G., Gowen, A.: The hype in spectral imaging. J. Spectral Imaging **9** (Feb 2020). https://doi.org/10.1255/jsi.2020.a4

24. Pu, Y.Y., Feng, Y.Z., Sun, D.W.: Recent Progress of Hyperspectral Imaging on Quality and Safety Inspection of Fruits and Vegetables: A Review. Compr. Rev. Food Sci. Food Saf. **14**(2), 176–188 (Mar 2015). https://doi.org/10.1111/1541-4337.12123

25. Qiao, S., Tian, Y., Gu, W., He, K., Yao, P., Song, S., Wang, J., Wang, H., Zhang, F.: Research on simultaneous detection of ssc and fi of blueberry based on hyperspectral imaging combined ms-spa. Engineering in Agriculture, Environment and Food **12**(4), 540–547 (2019). https://doi.org/10.1016/j.eaef.2019.11.006

26. Ramanan, A.: Taking a bite out of food waste **32**(10), 48–51 (oct 2019). https://doi.org/10.1088/2058-7058/32/10/32

27. Riccioli, C., Pérez-Marín, D., Garrido-Varo, A.: Optimizing spatial data reduction in hyperspectral imaging for the prediction of quality parameters in intact oranges. Postharvest Biology and Technology **176**, 111504 (2021). https://doi.org/10.1016/j.postharvbio.2021.111504

28. Savitzky, Abraham. Golay, M.J.E.: Smoothing and Differentiation of Data by Simplified Least Squares Procedures. Analytical Chemistry **36**, 709–717 (1964). https://doi.org/10.1021/ac60214a047

29. Wang, Y.W., Reder, N.P., Kang, S., Glaser, A.K., Liu, J.T.C.: Multiplexed Optical Imaging of Tumor-Directed Nanoparticles: A Review of Imaging Systems and Approaches. Nanotheranostics **1**(4), 369 (2017). https://doi.org/10.7150/ntno.21136

30. Zhu, H., Chu, B., Fan, Y., Tao, X., Yin, W., He, Y.: Hyperspectral Imaging for Predicting the Internal Quality of Kiwifruits Based on Variable Selection Algorithms and Chemometric Models. Sci. Rep. **7**(7845), 1–13 (Aug 2017). https://doi.org/10.1038/s41598-017-08509-6